

Self-Controlled Switchable Current Sharing Path for Multi-Receiver Wireless Power Transfer Systems

Ahmet Halis Sabırı, Enes Ayaz, Ozan Keysan

Abstract—This paper presents a self-controlled current balancing method with a switchable current sharing path for multi-receiver (multi-Rx) wireless power transfer (WPT) systems. Conventional methods utilize a continuous current-sharing path, but it has drawbacks, such as higher circulation current and lower efficiency with strong misalignment or under fault. Therefore, it is challenging to use modular structures to achieve misalignment-tolerant and highly-efficient systems in high-power applications. In the proposed system, the current sharing path automatically turns on within a pre-defined misalignment ratio and turns off under fault or strong misalignment conditions. Also, the proposed system just has passive elements, so an Rx-side controller and gate drives for the switches are not required. An experimental setup of the 1Tx-2Rx system is presented for different misalignment and fault conditions. In the proposed system, it is observed that 140 W output power is transferred with an efficiency of %71.85 under even a case of %70 misaligning of one module. It also achieved, compared to the conventional current sharing path, a 125% and a 150 % efficiency increase in the cases of strong misalignment and fault, respectively.

Index Terms—Wireless power transfer, multi-receiver, current balancing, modular structure

I. INTRODUCTION

Inductive power transfer (IPT) systems are becoming increasingly popular in industrial applications since they offer several benefits over traditional wired power systems [1], [2]. They improve safety, portability, reliability, and efficiency [3]–[5]. Although IPT systems are suitable for low-power consumer electronic products, industrial applications have some challenges, such as efficiency and misalignment tolerance. Therefore, modular structure in IPT systems, which is shown in Fig. 1, is proposed in the literature.

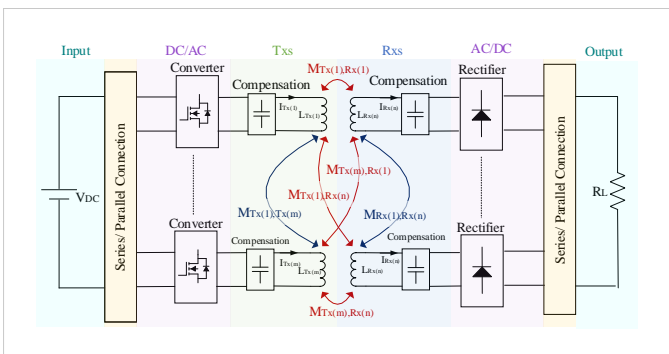


Fig. 1. The circuit diagram of a modular inductive power transfer system.

Ahmet Halis Sabırı, Enes Ayaz, and Ozan Keysan are with the Department of Electrical and Electronics Engineering, Middle East Technical University, Ankara, Turkey. Ahmet Halis Sabırı is also working at ASELSAN Inc.

Corresponding Author: Ozan Keysan, keysan@metu.edu.tr

The modular structure allows the system to be easily customized and scaled to meet the application specific ratings [6]. Besides, the connection of modules (parallel or series structures) allows utilizing the semiconductors with lower current or voltage ratings [7]. Moreover, modular structure simplifies thermal management and increases efficiency by sharing power and losses. Furthermore, they can be designed with built-in redundancy [8]. If one module fails, the system can continue to operate with the remaining modules, which increases reliability. However, modular coils are susceptible to slight misalignment due to mechanical movement in dynamic applications, and manufacturing tolerances [9]–[11]. Therefore, modular systems have power-sharing issue between the modules (Txs or Rxs). One drawback of the unbalanced power distribution is exceeding voltage and current ratings of the semiconductors. Another drawback is reduced efficiency due to power flowing dominantly from fewer modules, increasing ohmic losses. Further, due to these drawbacks, unequal power distribution causes early aging of the modules and reliability problems.

The unequal power distribution issue may occur in Tx modules or Rx modules. It can be solved in multi-Tx structures by just applying a control algorithm since Tx modules have active DC/AC converters. In [12], a d-q frame control is given in order to balance the current for parallel Tx's and minimize circulating current. In [13], multiphase Tx modules are used with a hybrid phase frequency control strategy. However, in order to reduce control complexity, passive methods are also proposed. In [14], coupled inductors with a cyclic cascade connection are proposed. In [15] and [16], a path is introduced to achieve passive and automatic current sharing. In [17], passive-impedance-matching by parallel connected additional inductance is introduced to achieve automatic current sharing for multi-Tx. The solution for Tx modules can also be applied for multi-Rx structures but Rx modules usually are made up of passive rectifiers. Therefore, implementing a control algorithm is not possible without additional hardware, which increases control complexity and cost. Hence, passive balancing methods gain more importance for Rx modules. In [18], it is proposed that detuning the receiver side is a viable option to reduce unbalance in addition to cross-coupling between the Rx modules. In [19], a middle-stage resonator is introduced to solve this power-sharing issue, and in this system, balanced power transfer is achieved even in the case of a fault. In [20], the current sharing path is introduced on the RX-side, similar to Tx-side. However, in the case of fault and strong misalignment, it is observed that the passive balancing method creates circulating currents and disturbs the fault tolerance.

In this paper, a new current balancing method for multi-Rx systems that is powered and controlled by the induced voltages of Rx coils without an additional controller and gate-drive circuitry is introduced to create a switchable current-sharing path between receiver coils. The proposed system avoids unbalanced power transfer between the receiver coils, and also, in the case of fault or strong misalignment, it disconnects the current sharing path by tracking the receiver coil voltages with self-control.

The remaining parts of the paper are as follows. Section II gives the system structure of a multi-receiver system. Section III defines the current sharing problem with a mathematical model. Section IV analyses the conventional current sharing path methods for misalignment and fault conditions. Section V introduces the proposed method. Section VI gives experimental validation.

II. SYSTEM STRUCTURE

The proposed system aims for a modular structure for WPT systems to achieve misalignment-tolerance and high efficiency. With misalignment, the coupling coefficient between Tx-Rx modules changes drastically. On the one hand, this change can reduce the transferred power, and a modular structure was already introduced to avoid it. On the other hand, the system's resonance frequency may also vary due to the change in the coupling coefficients. Since the series-series compensation topology gives load and coupling independent resonance frequencies, in the proposed system, series-series topology is chosen. However, series-series topology draws a short circuit current in the cases of no-load and zero coupling. The coupling between Tx and Rx may reduce almost to zero due to misalignment, which causes a short circuit current. Therefore, the proposed system should be designed so that a Tx module is coupled with at least two Rx modules in the aligned position. Therefore, even if one of the modules is decoupled, the Tx side sees a load and has non-zero coupling. Although, Tx and Rx modules can be connected in series or in parallel, in the proposed system, a parallel connection is used to increase efficiency.

As a representative example of the proposed system, a 1Tx-2Rx system, as shown in Fig. 3, is analyzed analytically. If higher power ratings are desired, the number of modules can be increased. These modules can be connected in series to decrease the voltage stress of the semiconductors or in parallel to decrease the current stress.

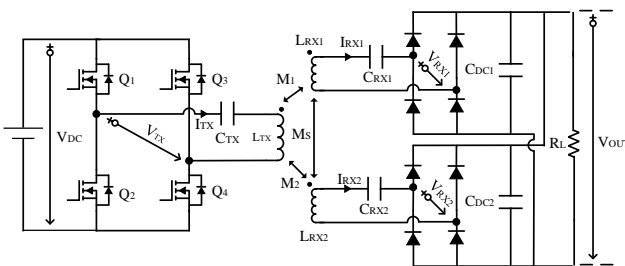


Fig. 2. The representation of 1Tx-2Rx series-series IPT system.

A. The System Parameters

The first harmonic approach of the 1Tx-2Rx system is given in Fig. 3.

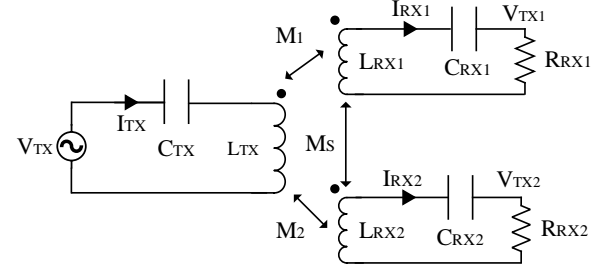


Fig. 3. First harmonic approach (FHA) model of the 1Tx-2Rx system.

The design parameters can be defined for a 1Tx-1Rx design, and later the Rx side can be divided into two parallel modules. The design methodology of 1Tx-1Rx series-series structures is well studied in the literature, and it is out of the topic of this paper. Therefore, the design steps in [21] are followed, and the parameters given in Table I are used.

TABLE I
SYSTEM PROPERTIES AND KEY PARAMETERS

Number of Tx modules	1
Number of Rx modules	2
Power Rating	125 W
Input Voltage (V_{in})	40 V _{DC}
Output Voltage (V_{out})	25 V _{DC}
Resonant Frequency	160 kHz
Tx-Rx Magnetic Coupling	0.20
Rx module Cross-Coupling	-0.03
Rx side Quality Factor (Q_{Rx})	2.25
Tx Inductance (L_{Tx})	43.6 μ H
Tx Capacitance (C_{Tx})	22 nF
Rx Inductance (L_{Rx})	8.8 μ H
Rx Capacitance (C_{Rx})	109 nF
Load Resistance (R_L)	5 Ω

III. PROBLEM DEFINITION AND MATHEMATICAL MODEL

Although, it is expected that parallel connected Rx modules have the same current. It is observed that all current is drawn from the module that has a higher coupling coefficient, even with a slight coupling difference. This is because the dominant module keeps the output voltage at its own voltage gain, and thus, the diodes of the recessive module are blocked. Fig. 4 shows the simulation results of receiver currents for the aligned and misaligned cases. For the misaligned case, coupling differences are kept at 10%, and it is observed that the current of the recessive module becomes zero.

This unbalanced current sharing can be modeled by unequal reflected module resistance using the first harmonic approach (FHA). The reflected resistance of a series compensated single-Rx can be calculated as in (1).

$$R_{RX} = \frac{8}{\pi^2} R_L \quad (1)$$

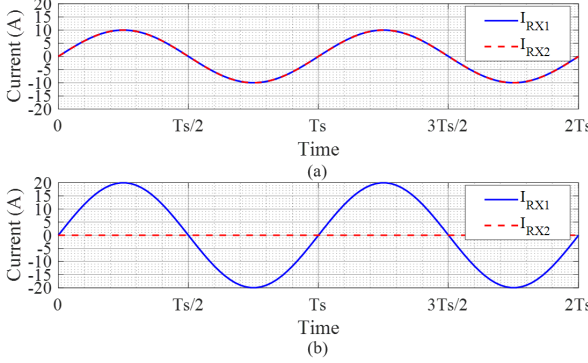


Fig. 4. Current waveforms of receivers in a) aligned and b) 10% misaligned cases of the 1Tx-2Rx system.

For the double-Rx system, the reflected resistances are doubled as in (2).

$$R_{RX(1)} = 2R_{RX}, R_{RX(2)} = 2R_{RX} \quad (2)$$

However, as the coupling coefficients between Tx and Rx differ, the reflected resistances change drastically compared to the balanced case. Nevertheless, it should be considered that the total reflected resistance is the same as in (3).

$$\frac{1}{R_{RX}} = \frac{1}{R_{RX1}} + \frac{1}{R_{RX2}} \quad (3)$$

The induced voltages of the Rx coils are calculated as in (4), which depends on the mutual inductance and Tx current. Besides, if the system operates at the resonant frequency, the output voltage of the receivers is equal to the induced voltage, and they should be equal in parallel connection as presented in (5).

$$\begin{aligned} V_{RX(1)_induced} &= j\omega M_{(1)} I_{TX} \\ V_{RX(2)_induced} &= j\omega M_{(2)} I_{TX} \end{aligned} \quad (4)$$

$$|V_{RX(1)}| = |V_{RX(2)}| = |V_{RX(1)_induced}| = |V_{RX(2)_induced}| \quad (5)$$

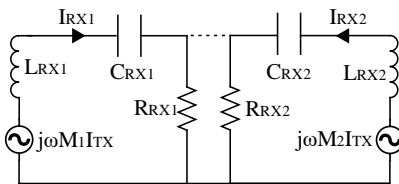


Fig. 5. The lumped circuit of the parallel connected modules with receiver series compensation.

In Fig. 5, the lumped circuit of the receiver side is presented. The module's voltages can be calculated as in (6) where $Z_{RX} = \frac{1}{j\omega C_{RX}} + j\omega L_{RX}$.

$$V_{RX(1)(2)} = R_{RX(1)(2)} \frac{j\omega M_{(1)(2)} I_{TX}}{Z_{RX} + R_{RX(1)(2)}} \quad (6)$$

Then, the equality condition of the module's voltages is obtained as in (7), and it is brought into a closed form, as given in (8) where α is defined as M_1/M_2 .

$$|R_{RX(1)} \frac{M_1}{Z_{RX} + R_{RX(1)}}| = |R_{RX(2)} \frac{M_2}{Z_{RX} + R_{RX(2)}}| \quad (7)$$

$$0 = ((\alpha^2 - 1)R_L^2 - |Z_S|^2)R_1^2 + 2R_L R_1 + (\alpha^2 - 1)|Z_S R_L|^2 \quad (8)$$

The quadratic equation in (8) can be solved, and the reflected resistance of the first module can be calculated as in (9).

$$\begin{aligned} R_{RX(1)} &= \frac{R_{RX} |Z_{RX}|^2}{(1 - \alpha^2)R_{RX}^2 + |Z_{RX}|^2} \\ &+ R_{RX} Z_{RX} \frac{\sqrt{|Z_{RX}|^2 \alpha^2 - R_{RX}^2 (1 - \alpha^2)^2}}{(1 - \alpha^2)R_{RX}^2 + |Z_{RX}|^2} \end{aligned} \quad (9)$$

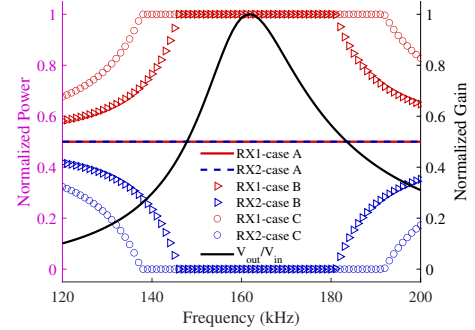


Fig. 6. The normalized power distribution of RX1 (the dominant module) and RX2 (the recessive module) for different alignment positions (Case-A: Aligned, Case-B: 10% Misaligned, Case-C: 20% Misaligned.) and the normalized gain of the WPT system.

The normalized power distributions of RX1 (the dominant module) and RX2 (the recessive module) are plotted in Fig. 6 as a function of the frequency for different alignment positions. The power distribution at the resonant frequency is susceptible, and total power is delivered by only one module, even if there is a slight change in the mutual inductance. The power-sharing becomes better as the operation frequency is moved away from the resonant frequency, but for this case, the gain of the WPT system is also decreasing, as given in Fig. 6. It means that the rated power cannot be achieved if the operation is moved away from the resonant frequency, even if the current is balanced.

IV. CURRENT-SHARING PATH ANALYSES

The current sharing path can be utilized to avoid unbalanced current sharing at frequencies close to the resonant frequency. The equivalent circuit of the 1Tx-2Rx system with the current sharing path is shown in Fig. 7. The impedances seen by the receiver inductances (Z_{Rx1} and Z_{Rx2}) can be calculated as in (10) with the assumption of that the self-inductances and compensation capacitors are equal.

$$Z_{Rx1} = Z_{Rx2} = Z_{Rx} = \frac{2}{j\omega C_{RX}} + R_{RX} \quad (10)$$

In this situation, it is observed that the reflected resistances to the receivers are independent of the mutual inductance,

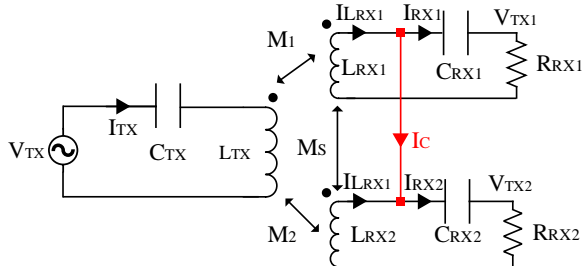


Fig. 7. FHA equivalent circuit of 1Tx-2Rx system with current sharing path (red line).

which guarantees that I_{Rx_1} is equal to I_{Rx_2} . However, coil currents differ from the receiver currents due to the circulation current, which can be calculated as in (11).

$$I_C = \frac{j\omega M_1 I_{TX} - j\omega M_2 I_{TX}}{L_{RX_1} + L_{RX_2}} \quad (11)$$

Due to the circulation current, the current sharing path may have some disadvantages in the cases of strong misalignment or faults. While a strong misalignment causes the quality factor of the system to change, short circuit or open circuit faults cause damage to the system and decrease its efficiency.

A. Misalignment Analysis

Thanks to the current balancing path, the resistances of the receivers are equal for misaligned cases. Thus, it guarantees that the diode rectifiers share the current, which decreases the ohmic losses. However, with increasing misalignment between the receivers, the gain characteristic of the WPT system changes due to the variation of the reflected resistance to the Tx side, which can be calculated as given in (12).

$$\begin{aligned} Z_{TX} &= \frac{\omega^2 M_1^2}{L_{RX_1} + \frac{Z_{RX_1} L_{LRX_2}}{Z_{RX_1} + L_{RX_2}}} + \frac{\omega^2 M_2^2}{L_{RX_2} + \frac{Z_{RX_2} L_{LRX_1}}{Z_{RX_2} + L_{RX_1}}} \\ &= \frac{\omega^2 (M_1^2 + M_2^2)}{L_{RX} + \frac{Z_{RX} L_{LRX}}{Z_{RX} + L_{RX}}} \end{aligned} \quad (12)$$

The normalized gains for several misaligned cases are plotted in Fig. 8. In the misaligned cases, the operating frequency should be changed to achieve the desired gain, and in this situation, it is observed that the phase of the Tx current (so power factor) changes, which increases the Tx current and decrease the efficiency as well.

Accordingly, for a specified misalignment, the current balancing path should be disconnected to increase the overall efficiency. The specified misalignment and the proposed switchable current balancing path will be discussed in Section V.

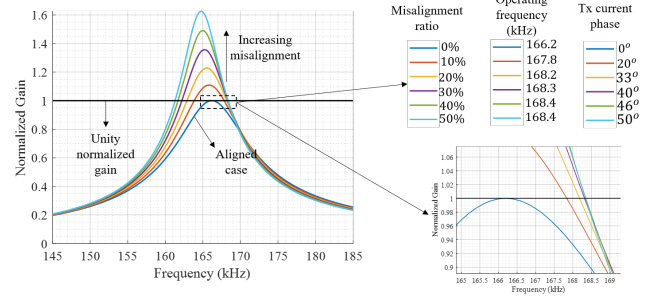


Fig. 8. The normalized gain of the WPT system for various misaligned cases and their operating frequencies and Tx current phases to achieve the unity normalized power.

B. Faulty Conditions

In healthy conditions within a specified misalignment, the current sharing path guarantees the balance current distribution of the receivers. However, the modular design should also provide a fault-tolerance, and the effect of the current sharing path under fault conditions should be investigated. A common fault in modular WPT is short-circuited coils. If one module is circuited, the other module also behaves like a short circuit due to the current sharing path. Which ruins the fault tolerance of the system. The only solution is to monitor coils, and disconnect the current-sharing path in the case of a fault.

V. THE PROPOSED METHOD

The main disadvantage of the current sharing path proposed in [20] is the fixed connection between the receivers. Under fault this connection causes high currents to flow through current sharing path. Therefore, a new current balancing method, where the circuit diagram is given in Fig. 9, is implemented with self-controlled switches to disconnect the current sharing path automatically.

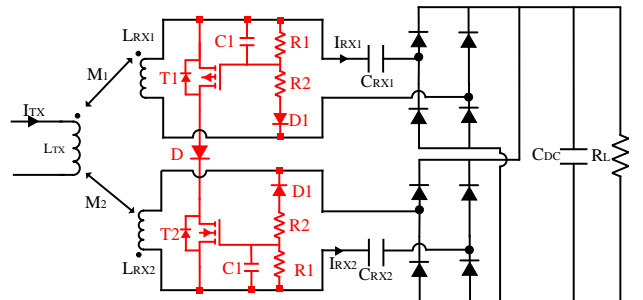


Fig. 9. The proposed 1Tx-2Rx IPT system with self-controlled current sharing path.

The proposed method has one switch for each receiver. These switches are ON if corresponding receiver coil's voltage is above a certain threshold. However, under fault or with strong misalignment, the corresponding switch automatically turns off blocking the current path.

Since the induced voltages are AC, bidirectional switches are required. PMOS and NMOS switches have body diodes which prevents them to block current in both directions. There

are several designs for bidirectional semiconductor switches but most of them require additional components or gate drivers [22]. To minimize the number of components, two semiconductor switches are used in such configuration that they can be controlled with the receiver coil voltages without any gate drivers. MOSFET switches are placed in a way that their body diodes are in same direction. An opposing diode is placed in between these MOSFET's to block the current flowing through the body diodes. This configuration can block current in both direction and conduct in one direction. Therefore, balancing operation is done only in one half cycle. To allow bidirectional current flow, the same switch set can also be connected in antiparallel way. However, it is seen that balancing even in one half cycle boosts recessive side coil voltage and ensures balanced operation in both half cycles.

Required gate voltages for the switches are generated from the receiver coils. However, gate voltage of a MOSFET must be referenced to the source pin of the devices. Since both body diodes must be in same direction, one of the switches is selected as NMOS and the other one as PMOS. With this selection, generated gate voltages can be referenced to the source pin of corresponding switches. To ensure continuous conduction during balancing operation, receiver coil voltage is rectified through a diode and a capacitor to create constant gate signal for the switch. Since MOSFET gate current is nearly zero, generated gate voltage does not impact the receiver. Magnitude of the gate voltages are adjusted by the resistors and limited with a zener protection diode. Resistors determine the misalignment tolerance.

A simulation setup is build to verify the operation of the design. Coupling of one receiver is changed during the simulation to observe the transient response. Limit for the misalignment is set to 50% with resistors as explained in the next section. As it can be seen in Fig. 10, switchable current sharing path is in conduction in 10% misaligned case and stops conducting at 55% misalignment. 10% misaligned receiver coil is shorted in the same simulation setup to observe the response in short circuited condition and results are presented in Fig. 11

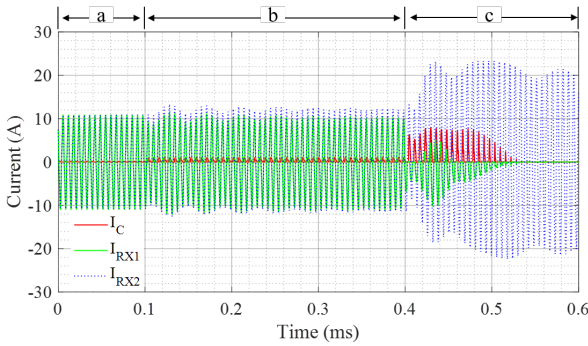


Fig. 10. Receiver coil currents and circulating current for (a) aligned, (b) 10% misaligned, (c) 55% misaligned case

A. Selection of the Resistors

Without balancing, the current of the recessive side is almost zero. Therefore, it can be assumed that receiver coil voltage

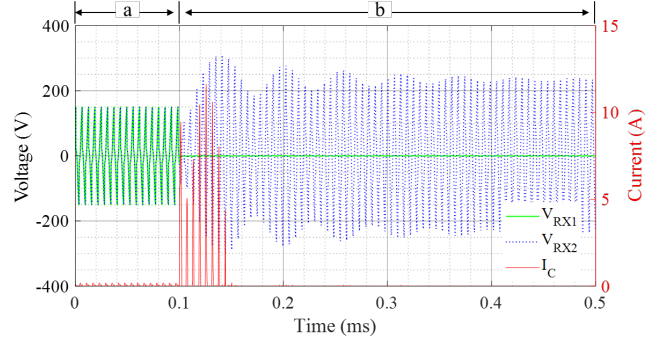


Fig. 11. Receiver coil voltages and circulating current before (a) and after (b) shorted receiver coil

of the recessive side has only induced voltage component from the transmitter side as in (4). However, transmitter current I_{TX_1} changes with misalignment due to change in transmitter side reflected resistance Z_{Tx} as given in (12). Assuming misalignment occurs in receiver #1, the mutual inductance can be replaced with misalignment ratio (β) defined as $\frac{M_2 - M_1}{M_2}$. Transmitter current is directly proportional with $1/Z_{Tx}$ in resonance frequency neglecting transmitter coil resistance. Therefore, using (12), ratio between the transmitter currents for the aligned case and the misaligned cases can be found as in (13).

$$\begin{aligned} \frac{T_{TX_{misaligned}}}{T_{TX_{aligned}}} &= \frac{2M_2^2}{(M_1^2 + M_2^2)} = \frac{2M_2^2}{((1-\beta)^2 M_2^2 + M_2^2)} \\ &= \frac{2}{(1-\beta)^2 + 1} \end{aligned} \quad (13)$$

Combining (4) and (13), induced voltage in receiver coil can be expressed in terms of aligned mutual inductance and aligned transmitter current as in (14).

$$V_{RX(i)} = j\omega(1-\beta)M_2I_{TX_{aligned}} \frac{2}{(1-\beta)^2 + 1} \quad (14)$$

Gate voltage (V_{GS}) of the MOSFETs are equal to the corresponding capacitor voltages. At steady-state, DC current component of the capacitor is zero. Therefore, DC current component of R_2 is equal to the DC current of R_1 . Current of R_1 can be found as (15):

$$I_{R1_{DC}} = \frac{V_{C_1}}{R_1} \quad (15)$$

DC current component of R_2 can be calculated with DC voltage component of R_2 . Since induced receiver coil voltage is sinusoidal and diode D_1 blocks negative half-cycle, DC voltage of R_2 can be found as in (16):

$$V_{R2_{DC}} = \frac{\hat{V}_{RX(1)} - V_F - V_{C_1}}{\pi} \quad (16)$$

$$I_{R2_{DC}} = \frac{V_{R2_{DC}}}{R_2} = I_{R1_{DC}} = \frac{V_{C_1}}{R_1} \quad (17)$$

Combining (14), (16) and (17):

$$\frac{V_{C_1}}{R_1} = \frac{\hat{V}_{RX(1)} - V_F - V_{C_1}}{\pi R_2} \quad (18)$$

$$= \frac{\omega M_{(2)} I_{TX_{aligned}} \frac{2\sqrt{2}(1-\beta)}{(1-\beta)^2 + 1} - V_F - V_{C_1}}{\pi R_2}$$

Where V_F is the forward voltage drop of D_1 . To find the resistor ratio for a given misalignment limit, $V_{C_1} = V_{GS}$ in (18) can be set to $V_{GS(th)}$ to turn off the MOSFET at that point. The final form is then found as in (19).

$$\frac{R_1}{R_2} = \frac{\pi V_{GS(th)}}{(\omega M_{(2)} I_{TX} \frac{2\sqrt{2}(1-\beta)}{(1-\beta)^2 + 1}) - V_F - V_{GS(th)}} \quad (19)$$

VI. EXPERIMENTAL VALIDATION

An experimental setup of the 1Tx-2Rx system is established, as shown in Fig. 12.

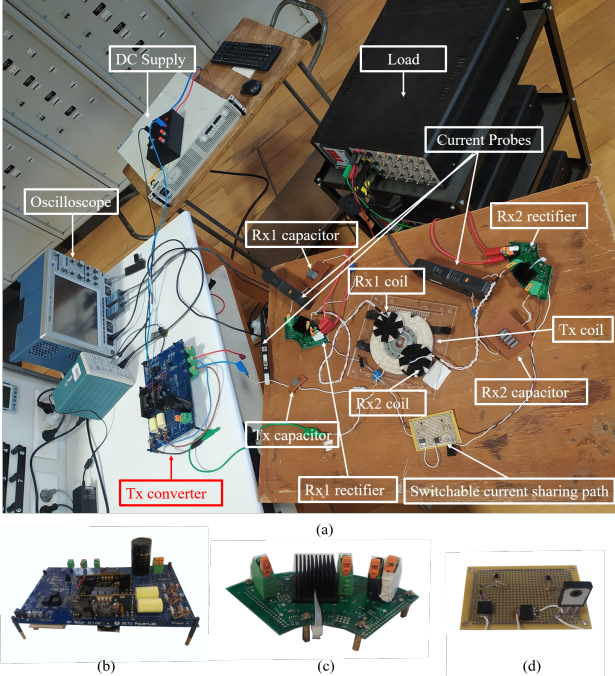


Fig. 12. Experimental setup. a) The overall structure of the test setup. b) Close view of the Tx-side converter. c) Close view of the Rx-side rectifier. d) Close view of the switchable current sharing path circuit.

Firstly, the system is tested with aligned and misaligned cases without the current sharing path. Then, the tests above are repeated with the proposed switchable current sharing path. After that, the proposed and conventional systems are tested under strong misalignment and short-circuit fault cases. Finally, the efficiency measurements are taken for all these conditions to compare the proposed and conventional systems.

A. Tests of 1Tx-2Rx system without current balancing

The receiver currents are shown in Fig. 13. for aligned and misaligned (40%) cases. As expected, the current of the recessive module is almost zero in the case of misalignment without the current sharing path.

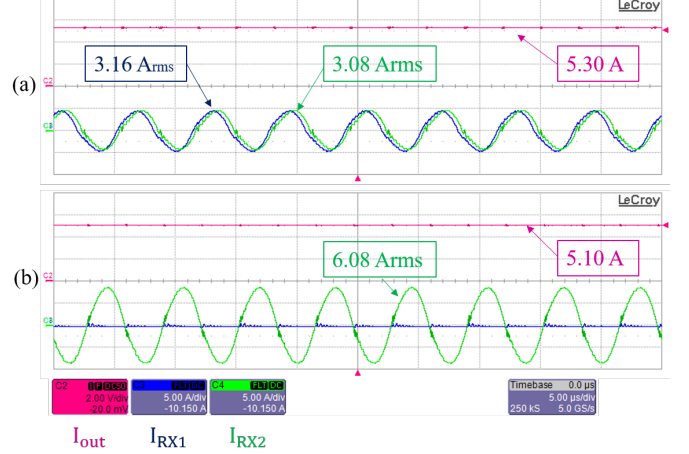


Fig. 13. Receiver coils and output currents. a) Aligned case. b) 40% misaligned case.

B. Tests of 1Tx-2Rx system with conventional and proposed current balancing methods

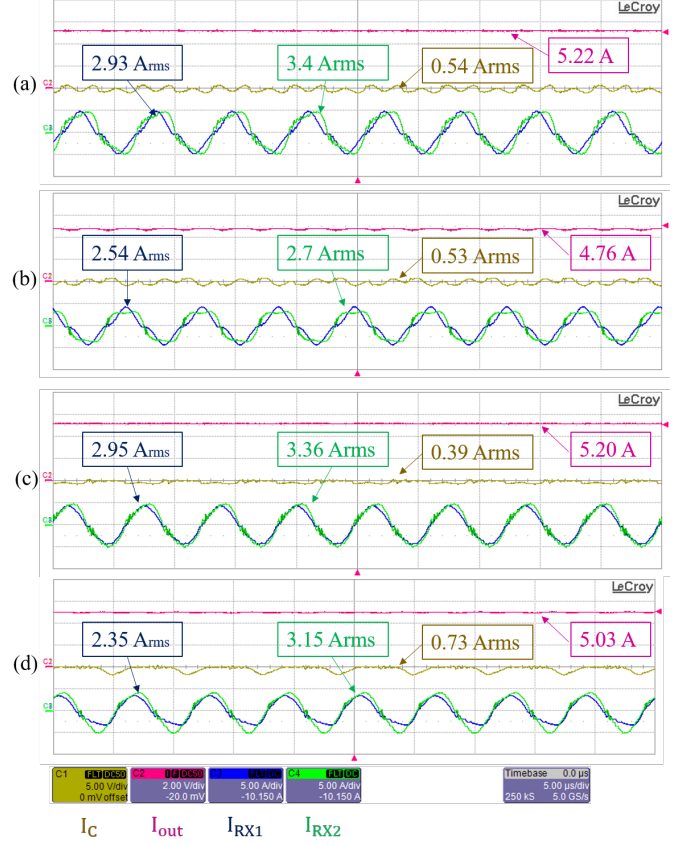


Fig. 14. Receiver coils, circulating, and output currents. a) Conventional current sharing path with the aligned case. b) Conventional current sharing path with a 40% misaligned case. c) The proposed current sharing path with the aligned case. d) The proposed current sharing path with a 40% misaligned case.

The receiver currents are shown in Fig. 14. for aligned and misaligned (40%) cases with the conventional and proposed current sharing paths. With the introduction of the current sharing path, the receiver current gets closer to each other. However, a circulation current exists, which also creates some higher-order harmonics. Further, in the proposed system, the efficiency is lower than the conventional current-sharing path due to voltage drops on the MOSFETs and the diode.

C. Tests of the 1Tx-2Rx system under strong misalignment and short circuit fault

The receiver currents are shown in Fig. 15 and Fig. 16 for the strong misalignment (%70) and short circuit faults with conventional and proposed current sharing paths.

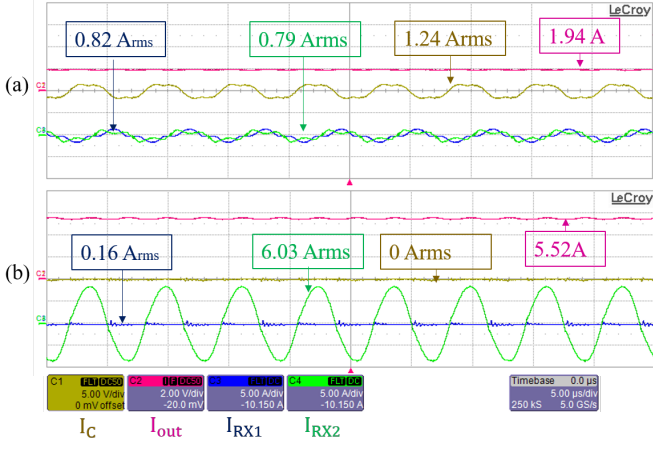


Fig. 15. Receiver coils, circulating, and output currents for strong misalignment. a) Conventional system. (For the conventional system, the input voltage is halved in order to avoid the high-circulating current.) b) The proposed method.

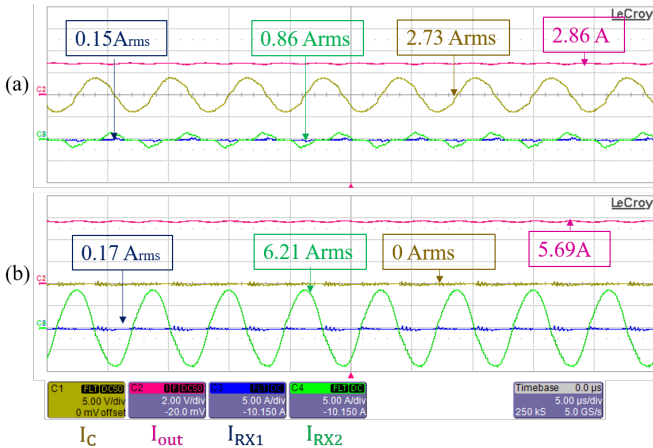


Fig. 16. Receiver coils, circulating, and output currents for short circuit fault. a) Conventional system. b) The proposed method.

In the conventional system, for strong misalignment, the circulating current keeps rising, which decreases the efficiency. Besides, under short-circuit, the healthy module also behaves like short-circuit, and the output power decreases as well. When the proposed method detects a strong misalignment or

a short-circuit fault, the current sharing path is instantly disconnected. Therefore, efficiency increases, and output power remains constant compared to healthy conditions.

D. Efficiency Comparison

The efficiencies of the aligned and misaligned cases are compared in Table II for systems-I (without a current sharing path), systems-II (with the conventional current sharing path), and the proposed system (with a switchable current sharing path). The efficiencies of the conventional and proposed system are given in Table III for the strong misalignment and a short-circuit fault.

TABLE II
EFFICIENCIES FOR THE ALIGNED AND MISALIGNED CASES.

	Efficiency (%)		Output Power (W)	
	Aligned	Misaligned	Aligned	Misaligned
System-I	73.6 %	67.2 %	136.2 W	130.3 W
System-II	71.8 %	73.78%	134.68 W	103.17 W
The proposed system	71.09 %	73.59 %	133.80 W	114.48 W

TABLE III
EFFICIENCIES FOR THE STRONG MISALIGNMENT CASE AND SHORT CIRCUIT FAULT.

	System-II	The proposed system
	Strong Misalignment	Efficiency (%)
Strong Misalignment	57.09 %	71.85 %
Short Circuit	46.97 %	71.25 %
Short Circuit	16.29 W	141.02 W
Short Circuit	37.48 W	150.47 W

It is concluded that although the proposed system efficiencies are slightly lower than the other systems for the aligned and misaligned case, the efficiencies become better in the case of strong misalignment and short-circuit fault. Further, by disconnecting the current sharing path, the proposed system is able to operate in fault conditions without system damage.

VII. CONCLUSION

In this paper, a new switchable current sharing path for multi-receiver (multi-Rx) wireless power transfer (WPT) systems is presented. The current sharing path is analyzed mathematically, and it is observed that the circulation current is increasing to dangerous levels in cases of strong misalignment and fault. Therefore, a self-controlled switchable current-sharing path is introduced to disconnect the path for these cases. The proposed system was tested under different conditions with an experimental setup of a 1Tx-2Rx series-series compensated WPT system. It was observed that the efficiency of the system is increased by the proposed method in short-circuit fault and strong misalignment compared to the conventional system. Moreover, it was observed that the system fault tolerance is increased by isolating the faulty modules (by disconnecting the current sharing path). Although the proposed method is investigated and implemented with a 1Tx-2Rx system, it can be expanded to any number of multiple receivers. Accordingly, with the proposed method, a modular

system, which can be scaled according to the desired power level, can be achieved, which is both misalignment-tolerant and efficient.

REFERENCES

- [1] G. A. Covic and J. T. Boys, "Modern trends in inductive power transfer for transportation applications," *IEEE Journal of Emerging and Selected Topics in Power Electronics*, vol. 1, no. 1, pp. 28–41, 2013.
- [2] Q. Deng, Z. Li, J. Liu, S. Li, D. Czarkowski, M. K. Kazimierczuk, H. Zhou, and W. Hu, "Multi-inverter phase-shifted control for ipt with overlapped transmitters," *IEEE Transactions on Power Electronics*, vol. 36, no. 8, pp. 8799–8811, 2021.
- [3] Y. Zhang, S. Chen, X. Li, and Y. Tang, "Design methodology of free-positioning nonoverlapping wireless charging for consumer electronics based on antiparallel windings," *IEEE Transactions on Industrial Electronics*, vol. 69, no. 1, pp. 825–834, 2022.
- [4] X. Qu, H. Chu, S.-C. Wong, and C. K. Tse, "An ipt battery charger with near unity power factor and load-independent constant output combating design constraints of input voltage and transformer parameters," *IEEE Transactions on Power Electronics*, vol. 34, no. 8, pp. 7719–7727, 2019.
- [5] S. Y. R. Hui and W. W. C. Ho, "A new generation of universal contactless battery charging platform for portable consumer electronic equipment," *IEEE Trans. Power Electron.*, vol. 20, no. 3, pp. 620–627, 2005.
- [6] H. Chen, Z. Qian, R. Zhang, Z. Zhang, J. Wu, H. Ma, and X. He, "Modular four-channel 50 kw wpt system with decoupled coil design for fast ev charging," *IEEE Access*, vol. 9, pp. 136083–136093, 2021.
- [7] H. Zhou, J. Chen, Q. Deng, F. Chen, A. Zhu, W. Hu, and X. Gao, "Input-series output-equivalent-parallel multi-inverter system for high-voltage and high-power wireless power transfer," *IEEE Transactions on Power Electronics*, vol. 36, no. 1, pp. 228–238, 2021.
- [8] H. Hao, G. A. Covic, and J. T. Boys, "A parallel topology for inductive power transfer power supplies," *IEEE Trans. Power Electron.*, vol. 29, no. 3, pp. 1140–1151, 2014.
- [9] G. Ning, K. Zhao, and M. Fu, "A passive current sharing method for multitransmitter inductive power transfer systems," *IEEE Transactions on Industrial Electronics*, vol. 69, no. 5, pp. 4617–4626, 2022.
- [10] H. Hu, S. Duan, T. Cai, and P. Zheng, "A current-sharing compensation method for high-power-medium-frequency coils composed of multiple branches connected in parallel," *IEEE Transactions on Industrial Electronics*, vol. 69, no. 5, pp. 4637–4651, 2022.
- [11] G. Ke, Q. Chen, W. Gao, S.-C. Wong, C. K. Tse, and Z. Zhang, "Research on ipt resonant converters with high misalignment tolerance using multicoil receiver set," *IEEE Transactions on Power Electronics*, vol. 35, no. 4, pp. 3697–3712, 2020.
- [12] H. He, Y. Liu, B. Wei, C. Jiang, S. Wang, X. Wu, and B. Jiang, "Circulating current suppression and current sharing strategy for parallel ipt system based on d-q synchronous rotating frame," *CSEE Journal of Power and Energy Systems*, pp. 1–14, 2022.
- [13] M. Bojarski, E. Asa, K. Colak, and D. Czarkowski, "Analysis and control of multiphase inductively coupled resonant converter for wireless electric vehicle charger applications," *IEEE Transactions on Transportation Electrification*, vol. 3, no. 2, pp. 312–320, 2017.
- [14] Q. Deng, J. Liu, D. Czarkowski, W. Hu, and H. Zhou, "An inductive power transfer system supplied by a multiphase parallel inverter," *IEEE Transactions on Industrial Electronics*, vol. 64, no. 9, pp. 7039–7048, 2017.
- [15] G. Ning, S. Wang, G. Zheng, Y. Liu, and M. Fu, "A novel passive current sharing method for a two-transmitter one-receiver wpt system," in *2020 IEEE 9th International Power Electronics and Motion Control Conference (IPEMC2020-ECCE Asia)*, 2020, pp. 985–990.
- [16] G. Ning, K. Zhao, and M. Fu, "A passive current sharing method for multitransmitter inductive power transfer systems," *IEEE Transactions on Industrial Electronics*, vol. 69, no. 5, pp. 4617–4626, 2022.
- [17] H. Wang, Y. Chen, and Y.-F. Liu, "A passive-impedance-matching technology to achieve automatic current sharing for a multiphase resonant converter," *IEEE Transactions on Power Electronics*, vol. 32, no. 12, pp. 9191–9209, 2017.
- [18] H. Polat, E. Ayaz, O. Altun, and O. Keysan, "Balancing of common dc-bus parallel-connected modular inductive power transfer systems," *IEEE Journal of Emerging and Selected Topics in Power Electronics*, vol. 10, no. 2, pp. 1587–1596, 2022.
- [19] E. Ayaz, O. Altun, H. Polat, and O. Keysan, "Fault tolerant multi-tx/multi-rx inductive power transfer system with a resonator coil," *IEEE Journal of Emerging and Selected Topics in Power Electronics*, vol. 11, no. 1, pp. 1272–1284, 2023.
- [20] G. Ning, P. Zhao, R. He, and M. Fu, "A novel passive current sharing method for a two-receiver-coil ipt system," in *2020 IEEE PELS Workshop on Emerging Technologies: Wireless Power Transfer (WoW)*, 2020, pp. 354–357.
- [21] O. Altun, E. Ayaz, H. Polat, and O. Keysan, "A modular inductive power transfer system for synchronous machine field excitation," in *2022 Wireless Power Week (WPW)*, 2022, pp. 476–481.
- [22] H. Dai, R. A. Torres, T. M. Jahns, and B. Sarlioglu, "Characterization and implementation of hybrid reverse-voltage-blocking and bidirectional switches using wbg devices in emerging motor drive applications," in *2019 IEEE Applied Power Electronics Conference and Exposition (APEC)*, 2019, pp. 297–304.